INTEGRATED DOPPLER CORRECTION TO TWSTFT USING ROUND-TRIP MEASUREMENT

Yi-Jiun Huang[1], Wen-Hung Tseng[1,2], and Shinn-Yan Lin[1]
[1]Telecommunication Laboratories (TL), Chunghwa Telecom, Taiwan
12, Lane 551, Min-Tzu Rd. Sec. 5, Yang-Mei, Taoyuan 32601, Taiwan
Tel: +886 3 4244783, Fax: +886 3 4245474, E-mail: *dongua@cht.com.tw*

[2]Institute of Photonics Technologies, National Tsing Hua University, Taiwan

Abstract

Diurnal variation is one of the significant instabilities in Two-Way Satellite Time and Frequency Transfer (TWSTFT) data. It is necessary to correct the diurnal variation for comparing the time-scale difference. We focus on the up-/downlink delay difference caused by satellite motion. In this paper, we propose to correct the TWSTFT data by using round-trip delay measurement. There are four laboratories: the National Institute of Information and Communications (NICT), Korea Research Institute of Standards and Science (KRISS), the National Time Service Center (NTSC), and TL, who join the TWSTFT network by using the NICT modem. Moreover, TL and NICT are continuing the DPN experiment. In the end, we investigate these TWSTFT data and the corrected data are performed.

INTRODUCTION

TWSTFT is one of the most precise technologies for comparing time-scale differences. Because two-way signal paths are highly reciprocal, it can achieve precise stability. There is another method, GPS Precise Point Positioning (GPS PPP), for comparing time-scale differences. However, GPS PPP's data need to be arranged by post-processing. It is an advantage that TWSTFT can perform time-scale differencing in real time.

However, TWSTFT faces a serious problem. Diurnal variation is one of the sources of instability and we find it significant in TWSTFT results. Since we do not find the diurnal from GPS PPP's results, it is impossible to evaluate the stability of time-scale differences by using TWSTFT. Many researchers work at finding the diurnal sources. **[1]** mentioned the variation of Sagnac residual according to ephemeris data, and corrected TWSTFT results for it. [2] proposed a correction method by adopting the troposphere delay model. **[3]** indicated and analyzed the possible instabilities, including environmental factors, ionosphere delay, satellite motion, and the satellite transponder. **[4]** further investigated the influence of ionosphere effect, satellite motion, and environmental conditions.

It is well-known that in order to keep the satellite static along the geostationary orbit, the satellite's operator has to adjust the position of satellite. The satellite will be set in slow motion and, thus, have a relative velocity with respect to the earth station. It causes the up-/downlink signal paths to be no longer

the same. That is called the integrated Doppler shift **[5]**. This paper is concerned with the correction based on the integrated Doppler shift. In this paper, we propose a method to calculate the integrated Doppler shift and then correct the TWSTFT results.

TWSTFT NON-RECIPROCITY

The following acronyms are defined according to ITU-R TF.1153-2 **[6]**. In this paper, we denote the time-scale difference between $1PPSTX_1$ and $1PPSTX_2$ as dt, and dt is either greater or less than zero. By the TWSTFT principle depicted in Fig. 1, at station 1, the 1PPS signal from station 2 will be received and the following measurement will be shown on the time-interval counter.

$$TI_1 = dt + TX_2 + SPU_2 + SCU_2 + SPT_2 + SPD_1 + SCD_1 + RX_1 \qquad (1)$$

The 1PPS signal from station 1 will be measured and shown at station 2.

$$TI_2 = -dt + TX_1 + SPU_1 + SCU_1 + SPT + SPD_2 + SCD_2 + RX_2 \qquad (2)$$

For simplicity, we combine the up-/downlink delay with the Sagnac correction. Let $SD_1 = SPD_1 + SCD_1$; then

$$TI_1 = dt + TX_2 + SU_2 + SPT_2 + SD_1 + RX_1 \qquad (3)$$

and

$$TI_2 = -dt + TX_1 + SU_1 + SPT_1 + SD_2 + RX_2 \qquad (4).$$

The time-scale difference is given by adding (3) with (4).

$$\begin{aligned} dt \;=\; & 0.5\times\left[TI_1 - TI_2\right] \\ +\; & 0.5\times\left\{\left[TX_1 - RX_1\right] - \left[TX_2 - RX_2\right]\right\} \\ +\; & 0.5\times\left\{\left[SU_1 - SD_1\right] - \left[SU_2 - SD_2\right]\right\} \\ +\; & 0.5\times\left[SPT_1 - SPT_2\right] \end{aligned} \qquad (5)$$

In the right-hand side of (5), the first term, $0.5\times\left[TI_1 - TI_2\right]$, represents the difference of counter readings, which we call TWSTFT data in this paper. The other terms address non-reciprocal factors. In this paper, we focus on the up-/downlink difference corresponding to the third term.

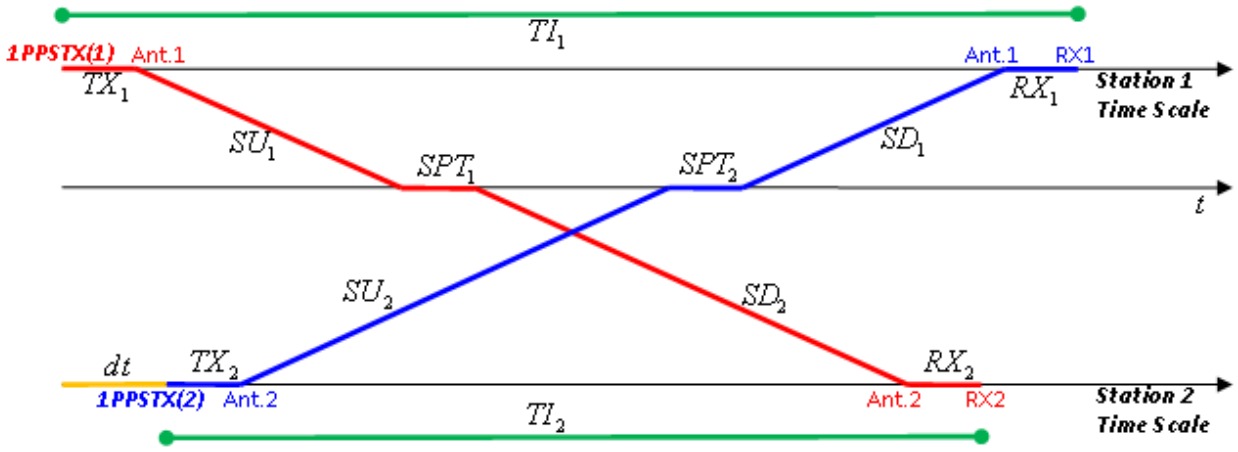

Fig. 1. Conceptual representation of time-interval counter readings, TI_1 and TI_2, along the two-way signal path.

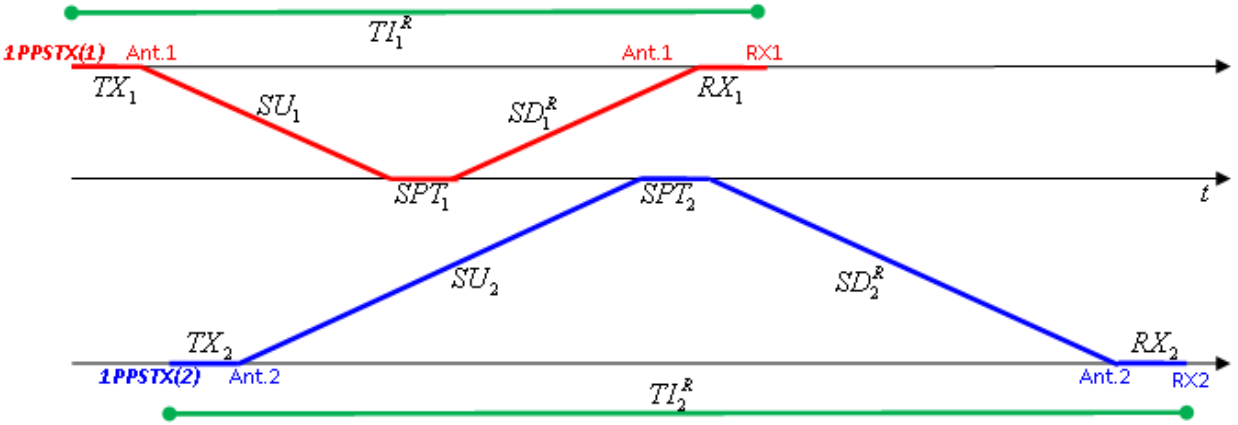

Fig. 2. Conceptual representation of time-interval counter readings (TI_1^R and TI_1^R) along the round-trip signal path.

NOTATION AND ASSUMPTION

Denote v_i as the rate of change of the distance $R_i(t)$ between earth station i and the satellite. In other words, v_i is regarded as the relative velocity, and has the following relationship with the relative distance $R_i(t)$.

$$R_i(t) = R_i(0) - v_i \cdot t \qquad (6)$$

Here, we assume v_i is fixed during 300 seconds, and has a plus sign when the satellite approaches the earth station. Because station 1 has to receive its 1PPS signal along the round-trip path, we further denote the round-trip downlink delay as SD_1^R, different from SD_1, which is the downlink delay along the two-way path. Figure 2 depicts the delay of each segment along the round-trip path. We ignore the

reference delay among all laboratories and the ionosphere delay at each site, because those have diurnal variations within hundreds of picoseconds, while the up-/downlink delay would have them in the hundreds of microseconds. We also ignore the transponder delay because that is not known. We further assume the 1PPS signal travels in free space; thus, the signal speed, defined as c, is a constant equal to 299,792,458 meters/second.

INTEGRATED DOPPLER SHIFT

This section is aimed at deriving the up-/downlink non-reciprocity caused by satellite motion. If the satellite is strictly geostationary, then the uplink and downlink delays are the same when the 1PPS signal travels along the round-trip path. That is,

$$SU_1 = SD_1^R = \frac{R_1(0)}{c} \qquad (7).$$

What happens if the satellite is in motion? First, we consider the 1PPS signal transmitted from station 1. We can get uplink delay SU_1 from (6).

$$SU_1 \cdot c = R_1(0) - SU_1 \cdot v_1 \qquad (8)$$

The satellite will receive and bypass the 1PPS signal from station 1 after SU_1 seconds. Along the round-trip path, the downlink delay is, thus, given by (6).

$$SD_1^R \cdot c = R_1(SU_1) - SD_1^R \cdot v_1 \qquad (9)$$

Along the two-way path, the downlink delay is also given by (6).

$$SD_2 \cdot c = R_2(SU_1) - SD_2 \cdot v_2 \qquad (10)$$

From (8) to (10), we can get the propagation delay of each segment in terms of relative distance and velocity.

$$SU_1 = \frac{1}{c + v_1} R_1(0) \qquad (11)$$

$$SD_1^R = \frac{c}{(c + v_1)^2} R_1(0) \qquad (12)$$

$$SD_2 = \frac{1}{c + v_2} R_2(0) - \frac{v_2}{(c + v_1)(c + v_2)} R_1(0) \qquad (13)$$

On the other hand, we can get the propagation delay when we consider the 1PPS signal transmitted from station 2.

$$SU_2 = \frac{1}{c+v_2} R_2(dt) \qquad (14)$$

$$SD_2^R = \frac{c}{(c+v_2)^2} R_2(dt) \qquad (15)$$

$$SD_1 = \frac{1}{c+v_1} R_1(dt) - \frac{v_1}{(c+v_1)(c+v_2)} R_2(dt) \qquad (16)$$

It is obvious that the propagation delays in (11) and (12) are different from those in (7). The difference caused by satellite motion is the so-called integrated Doppler shift. Therefore, from (11) to (16), the up-/downlink non-reciprocity that appears in the third term of (5) can be expressed in terms of relative distance and velocity.

$$0.5 \times \{[SU_1 - SD_1] - [SU_2 - SD_2]\} = \frac{v_2 R_1(0) - v_1 R_2(dt)}{2(c+v_1)(c+v_2)} \qquad (17)$$

(17) is called the integrated Doppler correction. To derive (17), we assume $R_1(dt) = R_1(0) - dt \cdot v_1$ is approximately equal to $R_1(0)$. It is reasonable that the satellite does not move rapidly within a few tenths of nanoseconds. In principle, $dt \cdot v_1$ is at the level of a few tenths of nanometers, and can be ignored if $R_1(0)$ is about 40,000 kilometers. In the next section, we will use the round-trip delay measurement to estimate the relative distances $R_1(0)$ and $R_2(dt)$, and relative velocities v_1 and v_2.

ESTIMATION USING ROUND-TRIP MEASUREMENT

The round-trip signal path is the path along which the 1PPS signal travels and returns between the earth station and the satellite. Only station 1 is considered in this section. From (8) and (9), the round-trip delay can be expressed as follows.

$$TI_1^R(0) := SU_1 + SD_1^R = \frac{(2c+v_1)}{(c+v_1)^2} R_1(0) \qquad (18)$$

We define $TI_1^R(k)$ as the round-trip delay measurement at time k when beginning to transmit the 1PPS signal at station 1. From (6), the round-trip delay measurement yields

$$TI_1^R(k) = \frac{(2c+v_1)}{(c+v_1)^2} R_1(k) = \frac{(2c+v_1)}{(c+v_1)^2} R_1(0) - \frac{(2cv_1+v_1^2)}{(c+v_1)^2} k \equiv a - bk \qquad (19).$$

Assume that (19) is a signal model and we observe $TI_1^R(k)$ for $k = 0,1,...,N-1$. Then, according to the least-squares approach, we can estimate a and b by minimizing the following equation.

$$J(a,b)=\sum_{k=0}^{N-1}\left(TI_1^R(k)-(a-b\cdot k)\right)^2 \qquad (20)$$

By differentiating with respect to a and b and setting the results to zero, we get

$$\begin{cases}\hat{a} &= \left(B\cdot\sum_{k=0}^{N-1}TI_1^R(k)-A\cdot\sum_{k=0}^{N-1}\left(k\cdot TI_1^R(k)\right)\right)\Big/\left(B-A^2\right)\\ \hat{b} &= \left(A\cdot\sum_{k=0}^{N-1}TI_1^R(k)-\sum_{k=0}^{N-1}\left(k\cdot TI_1^R(k)\right)\right)\Big/\left(B-A^2\right)\end{cases} \text{ where } \begin{cases}A &= \dfrac{n\cdot(n-1)}{2}\\ B &= \dfrac{n\cdot(n-1)\cdot(2n-1)}{6}\end{cases} \qquad (21).$$

From (19) and (21), we set $\hat{b}=\dfrac{2cv_1+v_1^2}{(c+v_1)^2}$ and then we can get the estimated relative velocity.

$$v_1=\frac{1-\sqrt{1-\hat{b}}}{\sqrt{1-\hat{b}}}c \qquad (22)$$

In the same way, we set $\hat{a}=\dfrac{2c+v_1}{(c+v_1)^2}R_1(0)$ and then we can get the estimated relative distance.

$$R_1(0)=\frac{(c+v_1)^2}{2c+v_1}\hat{a} \qquad (23)$$

We can follow the same procedure to derive v_2 and $R_2(dt)$.

DOPPLER EFFECT

In this section, we will verify that our derivation is identical to the Doppler Effect. If the satellite has a relative velocity with respect to an earth station, we will find the signal frequency observed at the satellite changed. The following formula is the Doppler Effect regarding all kinds of electromagnetic waves traveling in the free space:

$$\frac{\Delta f}{f}=\frac{v}{c} \qquad (24)$$

where we denote f, Δf and v as the signal frequency, the Doppler frequency, and the relative velocity. From this formula, we can get the frequency f_{SAT} observed at the satellite when station 1 transmits a 1PPS signal with frequency f_1.

$$f_{1,SAT}=\frac{(c+v_1)}{c}f_1 \qquad (25)$$

The 1PPS signal will be bypassed and reflected back to station 1 by the satellite, and we can measure the frequency $f_{1,round-trip}$ along the round-trip path at station 1.

$$f_{1,round-trip} = \frac{(c+v_1)}{c} f_{1,SAT} = \frac{(c+v_1)^2}{c^2} f_1 \qquad (26)$$

From this point of view, we verify our derivation by giving a short example. Since 1 second is the time interval of two consecutive 1PPS signals, by transmitting two consecutive 1PPS signals, we can receive them along the round-trip path and measure the time interval T' between them. From (19), we have

$$T_{1,round-trip} = 1 + TI_1^R(1) - TI_1^R(0) = 1 + \frac{(2c+v_1)}{(c+v_1)^2} R_1(1) - \frac{(2c+v_1)}{(c+v_1)^2} R_1(0) = \frac{c^2}{(c+v_1)^2} \qquad (27).$$

Equivalently, the observed frequency of 1PPS signal will be the inverse of the time interval T'. That is,

$$f_{1,round-trip} = \frac{1}{T_{1,round-trip}} = \frac{(c+v_1)^2}{c^2} \qquad (28).$$

This is the same as (26) when f_1 is set to 1 Hz, the frequency of 1PPS signal.

EXPERIMENT RESULTS

We have to receive the signals along the two-way and round-trip path at the same epoch, so it is necessary to use the multi-channel modem to get them. At present, the NICT modem is a multi-channel modem and is being employed among the Asia-Pacific TWSTFT links. Besides, Gotoh and Amagai **[7]** have developed a novel technique of TWSTFT with high precision. They use Dual PRN codes (DPN) signal as the 1PPS signal and design a GPU-based receiver by parallel signal processing. TL and NICT are now continuing the DPN experiment by which a round-trip delay measurement is also available. Both experiments are performing via the geostationary satellite IS-8 at 166E, and those data exchange though the Internet.

We regard the first terms in the right-hand side of (5) as TWSTFT data. The TWSTFT data from NICT modem and from DPN are depicted in Fig. 3. In Fig. 3, we can find that the diurnal variation exists in the NICT and in the DPN modem, and their tendencies are the same. However, their magnitudes of diurnal variation are not the same. It is evident that we have to use different multiple factors for correcting TWSTFT data. Practically, a factor of (17) will be used for correcting TWSTFT data.

The TWSTFT data and time deviation (TDEV) results are depicted in Figs. 4 to 6. The 2-month results are shown. We use (17) by a factor of 40 to correct TWSTFT data. Obviously, diurnal variation decreases, but does not vanish after TWSTFT data are corrected. There would be another source of instability that causes diurnal variation.

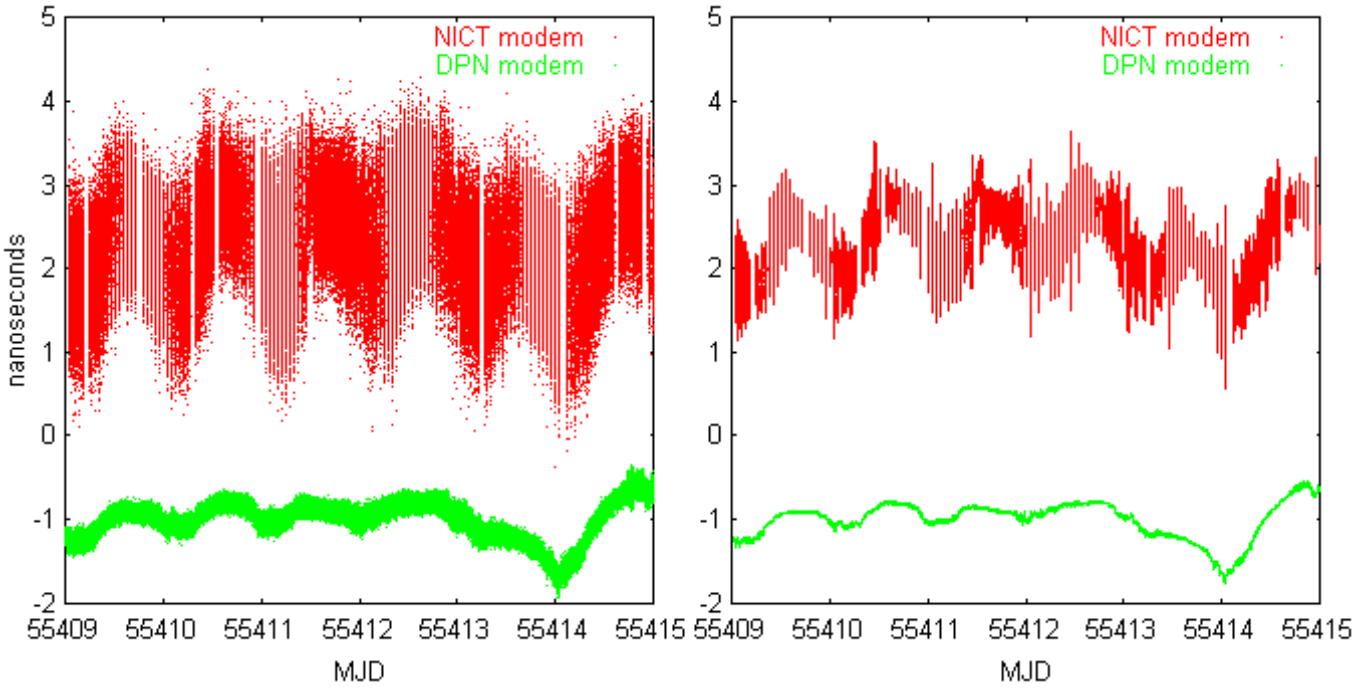

Fig. 3. TWSTFT data of NICT-TL link from the NICT modem (red line) and the DPN modem (green line) with averaging times of 1 second (left) and 300 seconds (right).

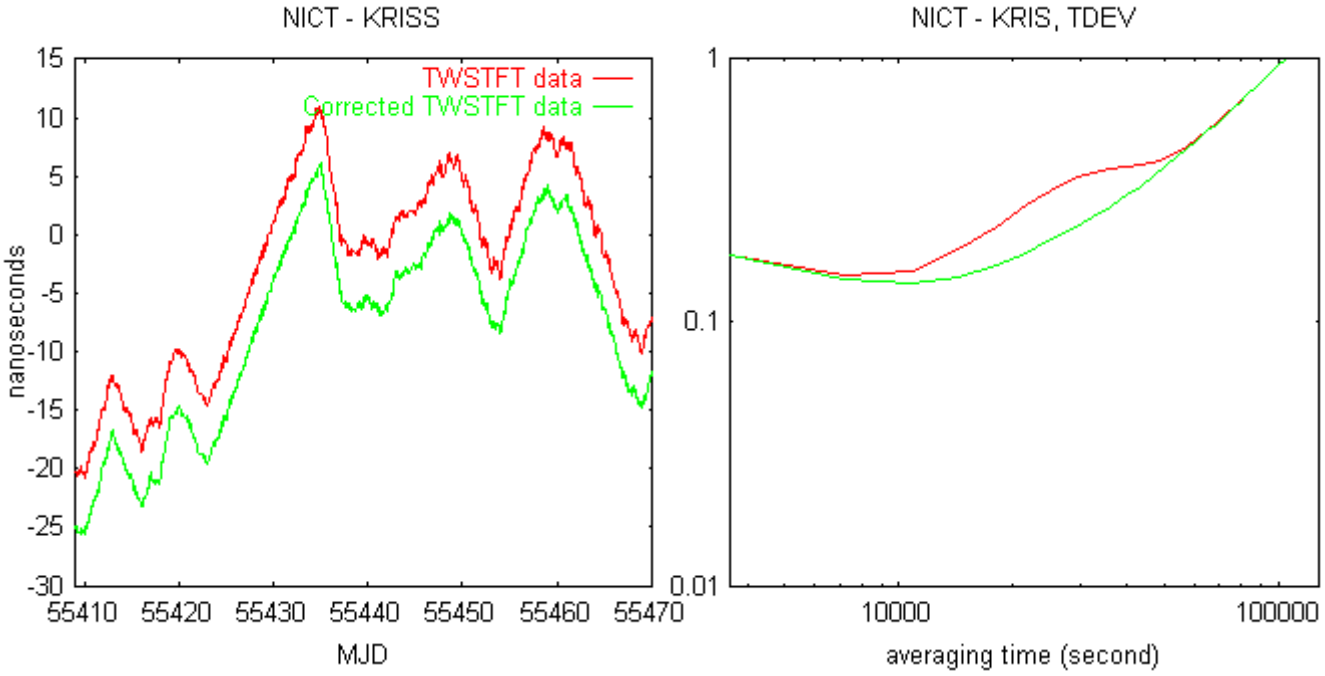

Fig. 4. TWSTFT data (left) and TDEV (right) of the NICT-KRISS link from the NICT modem.

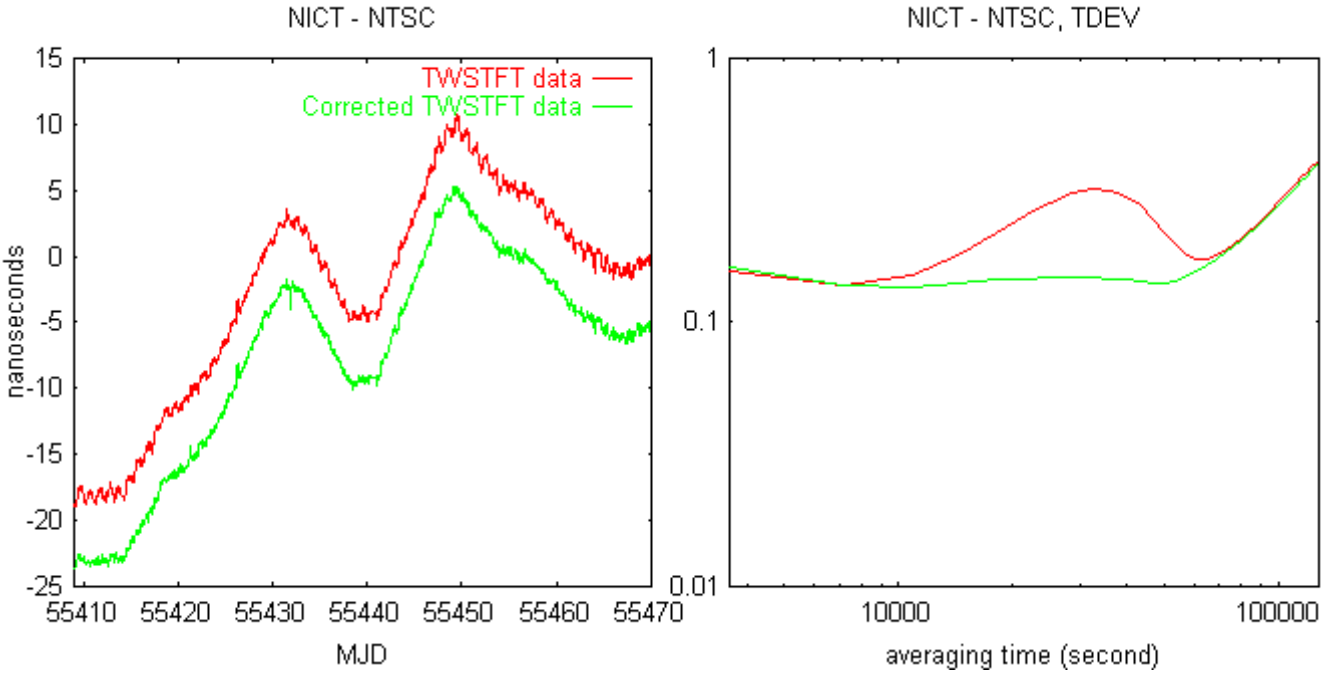

Fig. 5. TWSTFT data (left) and TDEV (right) of the NICT-NTSC link from the NICT modem.

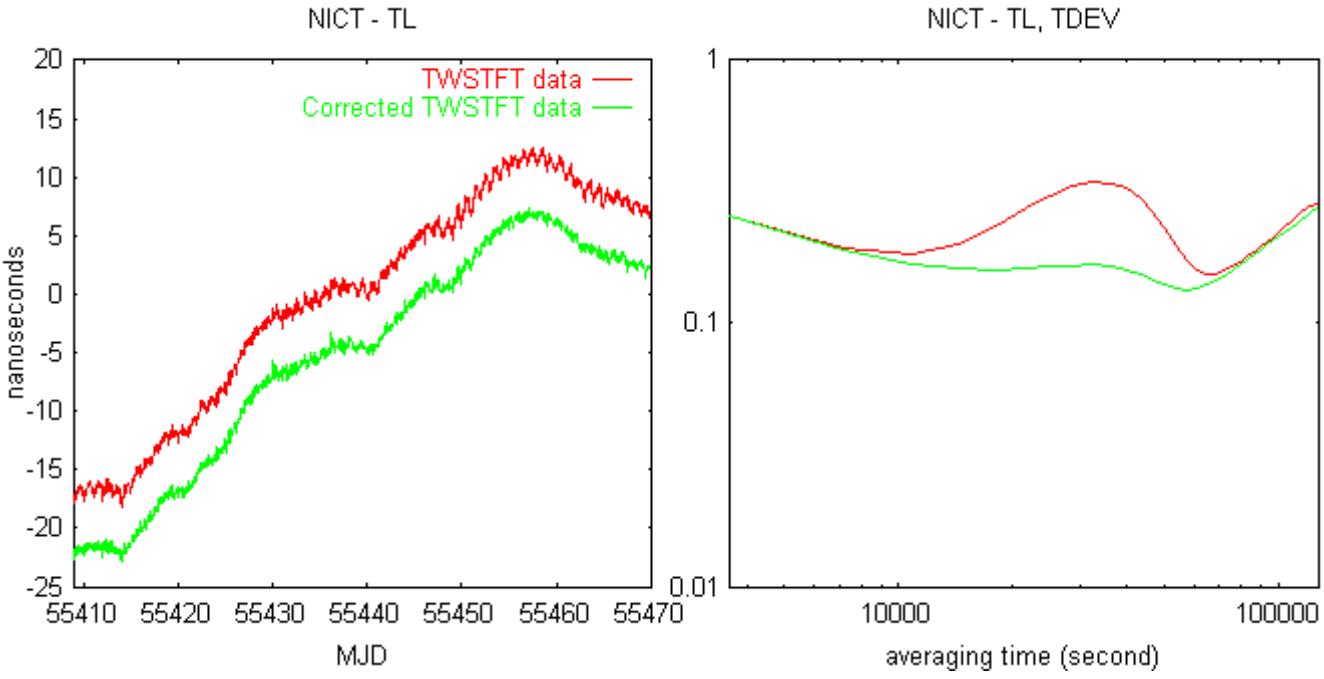

Fig. 6. TWSTFT data (left) and TDEV (right) of the NICT-TL link from the NICT modem.

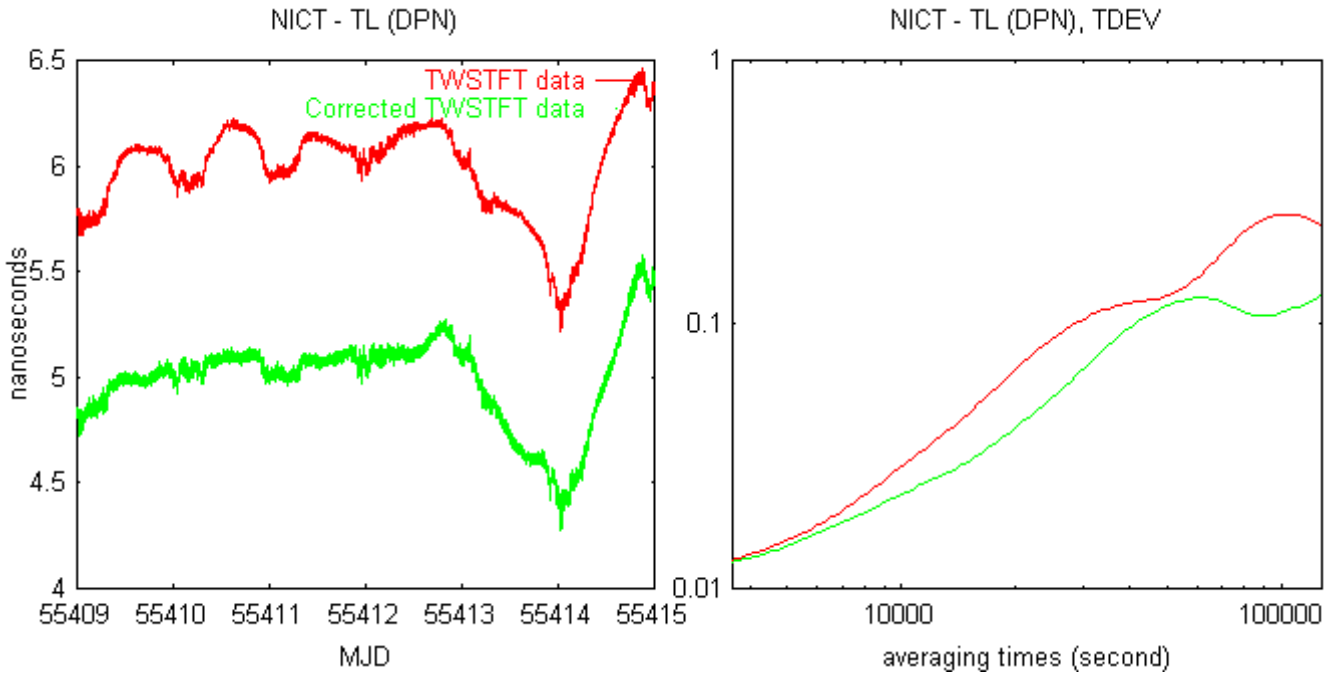

Fig. 7. TWSTFT data (left) and TDEV (right) of the NICT-TL link from the DPN modem.

Also, we show the 7-day TWSTFT data from the DPN modem in Fig 7. We find that the diurnal variation decreases with TWSTFT data corrected by a factor of 20.

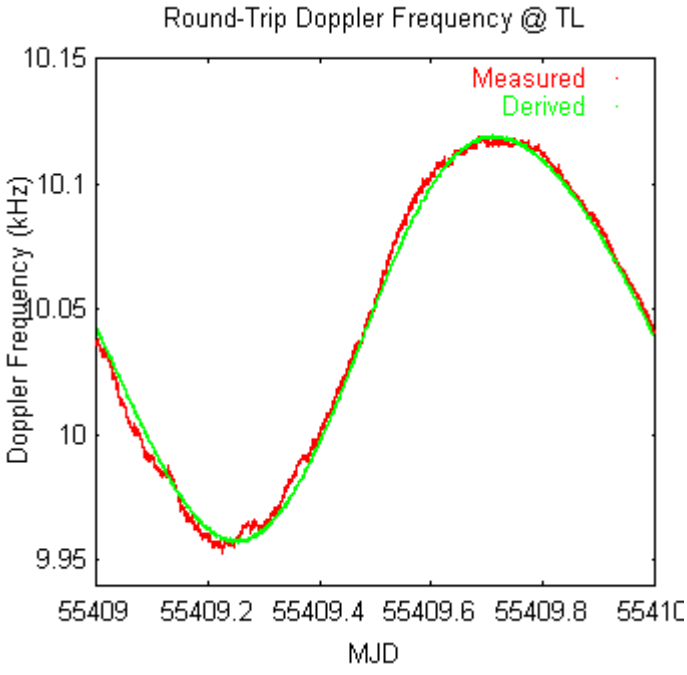

Fig. 8. Measured Doppler frequency (red line) and Doppler frequency derived by (24)-(26) (green line).

We verify that our derivation of relative velocity matches the theoretical Doppler frequency. Note that the transmit frequency is 14.164 GHz, the change of frequency is about 1753 MHz due to of transponder, and the receive frequency is 12.411 GHz. The measured frequency is recorded by the DPN modem. In Fig. 8, we can find that the two curves are in good agreement; thus, our derivation is meaningful and practical.

CONCLUSION

We use the integrated Doppler correction to improve TWSTFT stability, and the diurnal variation drops considerably. We consider that the integrated Doppler shift may be the dominant factor of diurnal variation even if diurnal variation does not vanish after correction. From experimental results, we find that the theoretical Doppler frequency is in good agreement with the measured Doppler frequency. We also find that integrated Doppler correction needs a multiple factor because the magnitudes of diurnal variation are not the same in the NICT and the DPN modems. It may be caused by signal waveform distortion, which we will investigate in the near future.

REFERENCES

[1] W. Tseng, K. Feng, S. Lin, H. Lin, Y. Huang, and C. Liao, 2010, *"Sagnac Effect and Diurnal Correction on Two-Way Satellite Time Transfer,"* in Proceedings of the 2010 Conference on Precision Electromagnetic Measurements (CPEM), 13-18 June 2010, Daejeon, Korea, pp. 436-437.

[2] D. Piester, A. Bauch, M. Fujieda, T. Gotoh, M. Aida, H. Maeno, M. Hosokawa, and S. H. Yang, 2008 *"Studies on Instabilities in Long-Baseline Two-Way Satellite Time and Frequency Transfer (TWSTFT) Including a Troposphere Delay Model,"* in Proceedings of the 39th Precise Time and Time Interval (PTTI) Systems and Applications Meeting, 27-29 November 2007, Long Beach, California, USA (U.S. Naval Observatory, Washington, D.C.), pp. 211-222.

[3] T. E. Parker and V. Zhang, 2005, *"Sources of Instabilities in Two-Way Satellite Time Transfer,"* in Proceedings of the 2005 Joint IEEE International Frequency Control Symposium (IFCS) and Precise Time and Time Interval (PTTI) Systems and Applications Meeting, 29-31 August 2005, Vancouver, British Columbia, Canada (IEEE 05CH37664C), pp. 745-751.

[4] M. Fujieda, T. Gotoh, M. Aida, J. Amagai, and H. Maeno, 2007, *"Long-Baseline TWSTFT between Asia and Europe,"* in Proceedings of the 38th Precise Time and Time Interval (PTTI) Systems and Applications Meeting, 5-7 December 2006, Reston, Virginia, USA (U.S. Naval Observatory, Washington, D.C.), pp. 499-504

[5] A. Gifford, R. A. Nelson, R. S. Orr, A. J. Oria, B. L. Brodsky, J. J. Miller, and B. Adde, 2007, *"Time Dissemination Alternatives for Future NASA Application,"* in Proceedings of the 38th Precise Time and Time Interval (PTTI) Systems and Applications Meeting, 5-7 December 2006, Reston, Virginia, USA (U.S. Naval Observatory, Washington, D.C.), pp. 319-328.

[6] ITU Radiocommunication Sector, *"The Operational Use of Two-Way Satellite Time and Frequency Transfer Employing PRN Code,"* ITU-R TF. 1153-2 (Geneva), 2003.

[7] T. Gotoh and J. Amagai, *"Two-Way Time Transfer with Dual Pseudo-Random Noise Code,"* in Proceedings of the 40th Precise Time and Time Interval (PTTI) Systems and Applications Meeting,

1-4 December 2008, Reston, Virginia, USA (U.S. Naval Observatory, Washington, D.C.), pp. 459-466.